Application of the predictor-corrector method to non-hydrostatic dynamics.

Jozef Vivoda, ALATNET-CHMI/SHMI

March 30, 2004

1 Introduction

The non-hydrostatic (NH) version of the limited area NWP model ALADIN is based on the Euler system of equations with the thin layer hypothesis (Bubnova (1995)). It is cast in the hybrid terrain following vertical coordinate based on hydrostatic pressure (Laprise (1992)).

Since ALADIN is a spectral model, the traditional Semi-Implicit (SI) scheme had to be implemented such that it retains stability by treating a linear constant coefficient Helmholtz equation in model spectral space. This appears, however, to be insufficient to control the short internal acoustic oscillations in the NH models. The traditional SI scheme is therefore unstable for both three and two-time level (2TL) schemes.

It was detected experimentally that the SI treatment must be applied also on the nonlinear residuals of three-dimensional divergence (Bubnová (1995)). Due to the non-linear character of three-dimensional divergence the additional SI treatment was performed by a simplified predictor-corrector (PC) algorithm around the existing Helmholtz solver. This stabilized the three-time level schemes but the 2TL SI semi-Lagrangian (SL) scheme remained unstable.

To stabilize the 2TL SI SL scheme, one of the two following methods has to be adopted. First method is to generalize the SI background state to be as close as possible to the actual atmospheric state in order to minimize the explicitly treated residuals (Golding (1992) and Qian (1998)). Using this approach a multidimensional non-symmetrical Helmholtz equation is obtained that has to be solved by an iterative solver in grid point space. This approach is not feasible in spectral models. Second approach assumes to retain the existing SI algorithm and to iterate the whole time stepping procedure around the existing linear constant coefficient Helmholtz solver. The obtained scheme is then an iterative approximation of the trapezoidal scheme (Cullen,2001). This approach is attractive for exploitation in spectral models and therefore it was decided to use it for NH ALADIN.

2 Formulation of the scheme

The 2TL SL ICI scheme is an iterative approximation of the Centred Fully Implicit (CFI) scheme

$$\frac{X_F^{t+\Delta t} - X_O^t}{\Delta t} = \frac{\mathcal{M}\left(X\right)_F^{t+\Delta t} + \mathcal{M}\left(X\right)_O^t}{2}. \tag{1}$$

The subscripts F resp. O represents the arrival point resp. the departure point of the trajectory.

The analytical solution of [1] is impossible, because $\mathcal{M}$ is a discretized nonlinear model and [1] represents the set of nonlinear equations. An iterative solution has to be applied.

To solve the problem, the nonlinear model is traditionally divided into a linear part and a nonlinear residual (Robert,1972) (linear part is denoted $\mathbf{L}$ and nonlinear residual $\mathcal{R}$ in the following text). $\mathbf{L}$ is treated implicitly in a direct way while $\mathcal{R}$ is treated explicitly. It yields the traditional 2TL SI scheme

$$\frac{X_F^{t+\Delta t} - X_O^t}{\Delta t} = \frac{\mathbf{L}_F^{t+\Delta t} + \mathbf{L}_O^t}{2} + \mathcal{R}_M^{t+\frac{\Delta t}{2}}. \tag{2}$$

A further implicit treatment of the terms included in $\mathcal{R}$ can be assured by the partial ICI scheme of Bubnová (1995)

$$\frac{X_F^{t+\Delta t(n)} - X_O^t}{\Delta t} = \frac{\mathbf{L}_F^{t+\Delta t(n)} + \mathbf{L}_O^t}{2} + (\mathcal{R} - \mathcal{Y})_M^{t+\frac{\Delta t}{2}} + \frac{\mathcal{Y}_F^{t+\Delta t(n-1)} + \mathcal{Y}_O^t}{2}. \tag{3}$$

Here, $\mathcal{Y}$ is the part of the nonlinear residual treated in the iterative manner and $X^{t+\Delta t(n)}$ is the model state after n-th iteration. In the first version of NH model ALADIN the term $\mathcal{Y}$ contained the compressibility term from the continuity equation. The aim of this work was to generalize the existing partial ICI scheme in order to treat the whole $\mathcal{R}$ in the iterative manner. Therefore we set $\mathcal{Y} = \mathcal{R}$. The ICI scheme then yields

$$\frac{X_F^{t+\Delta t(n)} - X_O^t}{\Delta t} = \frac{\mathbf{L}_F^{t+\Delta t(n)} + \mathbf{L}_O^t}{2} + \frac{\mathcal{R}_F^{t+\Delta t(n-1)} + \mathcal{R}_O^t}{2}. \tag{4}$$

The special case of [4] is the PC scheme with one iteration of a non-linear residual (n=1).

The SI linear model $\mathbf{L}$ has to be chosen carefully to assure effective convergence of the ICI scheme towards fully centered implicit scheme [1]. At the same time the SI scheme has to control fast moving acoustic and gravity modes. The traditionally $\mathbf{L}$ describes the small amplitude perturbations around isothermal, resting, hydrostatic reference state. However, this was found insufficient for NH dynamics. Bénard (2003) proposed the SI linear model $\mathbf{L}$ formulated with the two isothermal reference temperatures. This assures the effective control of instabilities associated with the thermal residuals. In NH dynamics the short acoustic modes require the SI temperature to be colder than any temperature in the domain in order to be stable. This is in contradiction with the requirement of gravitational modes, for which SI temperature has to be warmer than any temperature in the domain. Therefore new SI reference profile T_a^* has been introduced in the terms responsible for vertical propagation of acoustic waves while traditional SI temperature T^* is kept in the rest if the system.

The initial guess $X^{t+\Delta t(0)}$ has to be provided into the iterative procedure. The traditional 2TL SI SL scheme is used to calculate this guess as

$$\frac{X_F^{t+\Delta t(0)} - X_O^t}{\Delta t} = \frac{\mathbf{L}_F^{t+\Delta t(0)} + \mathbf{L}_O^t}{2} + \mathcal{R}_M^{t+\frac{\Delta t}{2}}.$$

where the nonlinear residual term at time instant $t + \frac{\Delta t}{2}$ is obtained by persistent prediction of state at time level t (NESC) or by second order extrapolation using states at time levels t and $t - \Delta t$ (SETTLS or Traditional) . It gives

NESC scheme (Cullen (2001))	$\mathcal{R}_M^{t+\frac{\Delta t}{2}} = \frac{1}{2}\left(\mathcal{R}_F^t + \mathcal{R}_O^t\right)$
SETTLS extrapolation (Hortal (1998))	$\mathcal{R}_M^{t+\frac{\Delta t}{2}} = \frac{1}{2}\left(2\mathcal{R}^t - \mathcal{R}^{t-\Delta t}\right)_O + \frac{1}{2}\mathcal{R}_F^t$
Traditional extrapolation	$\mathcal{R}_M^{t+\frac{\Delta t}{2}} = \frac{1}{2}\left(\frac{3}{2}\mathcal{R}^t - \frac{1}{2}\mathcal{R}^{t-\Delta t}\right)_O + \frac{1}{2}\left(\frac{3}{2}\mathcal{R}^t - \frac{1}{2}\mathcal{R}^{t-\Delta t}\right)_F$

The traditional extrapolation was found unstable in cases with strong jet-streams. Therefore Hortal (1998) developed the Stable Extrapolation for Two-Time Level Scheme (SETTLS), as a second order accurate extrapolation in time and space. The Non-Extrapolating SCheme (NESC) is even more stable than SETTLS, but it is less accurate. Its usage in ICI scheme is however beneficial since the accuracy is restored during the iterations and it requires less memory, because the model state $X^{t-\Delta t}$ is not used.

The same extrapolation problem exists in the computation of the trajectory wind used to determine the origin point. The wind is always computed consistently with the nonlinear residual.

The computation of trajectories and the evaluation of terms at the departure point is computationally the most expensive part of the SL ICI scheme. Therefore the two versions of the SL ICI scheme were developed.

1. The scheme with computation of trajectories only during the predictor using the second order extrapolation of wind (SETTLS or traditional extrapolation). The scheme is referred to as NOTR scheme.

2. The scheme with the re-interpolation of trajectories during the n-th iteration as

$$\vec{OF} = \Delta t \frac{1}{2} \left(\vec{v}_F^{t+\Delta t(n-1)} + \vec{v}_O^t \right). \tag{5}$$

   The guess $\vec{v}^{t+\Delta t(0)}$ is obtained using the NESC, SETTLS or traditional approach. The scheme is reffered to as FULL scheme.

3 Analyses of stability

The stability was analyzed using the method described by Simmons (1978), and Simmons and Temperton (1997). We replaced the non-linear problem

$$\frac{dX}{dt} = \mathcal{M}X. \tag{6}$$

by its linearised equivalent

$$\frac{\partial X}{\partial t} = \overline{\mathcal{M}}X. \tag{7}$$

The linear model $\overline{\mathcal{M}}$ is obtained by traditional linearization of $\mathcal{M}$ around the isothermal reference state $\overline{X}$ fully defined by its temperature $\overline{T}$ and the surface pressure $\overline{\pi_s}$.

Although some of the experiments in the following sections were performed using the bi-isothermal $\mathbf{L}$ model, the analysis of stability was performed with isothermal linear model ($T^* = T_a^*$).

The nonlinear residual is in the linear framework defined as $\overline{\mathcal{R}}.X = (\overline{\mathcal{M}} - \mathbf{L}).X$. When the states $\overline{X}$ and X^* are the same then $\overline{\mathcal{R}} = 0$ and the ICI scheme becomes the CFI scheme. When $\overline{X} \neq X^*$ then we can analyse two kinds of instability

1. the pressure instability ($\overline{\pi_s} \neq {\pi_s}^*$ and $\overline{T} = T^*$)

2. the temperature instability ($\overline{\pi_s} = {\pi_s}^*$ and $\overline{T} \neq T^*$)

The ICI scheme in the linear approximation can be written as

$$\text{predictor} \quad X^{t+\Delta t(0)} = C.X^t$$

$$\text{iterations} \quad X^{t+\Delta t(n)} = A.X^{t+\Delta t(n-1)} + B$$

Using this procedure we can calculate the amplification matrix of the n-th iteration as

$$X^{t+\Delta t(n)} = M_n X^t = \lambda_{M_n} X^t.$$

The analysed mode is stable if the growth rate $|\lambda_{M_n}| < 1$. The scheme should converge towards the solution of CFI scheme for which we can write

$$X_{CFI}^{t+\Delta t} = A.X_{CFI}^{t+\Delta t} + B. \tag{8}$$

The error of the n-th iteration is defined as $e^{t+\Delta t(n)} = X^{t+\Delta t(n)} - X_{CFI}^{t+\Delta t}$. The error growth is then given as

$$e^{t+\Delta t(n)} = Ae^{t+\Delta t(n-1)} = ... = A^n e^{t+\Delta t(0)} \tag{9}$$

The ICI scheme is convergent if the spectral radius of matrix A is less then unity. The spectral radius is defined as the maximum eigenvalue of A and the condition for convergence then yields

$$\rho(A) = max(|\lambda_A|) < 1. \tag{10}$$

Matrix A used in analyses is $A = (I - \frac{\Delta t}{2}\mathbf{L})^{-1}\frac{\Delta t}{2}\overline{\mathcal{R}}$.

We analysed the stability properties of ICI NESC scheme. We did not find any significant differences between the behavior of the ICI NESC scheme and ICI SETTLS scheme (resp. ICI traditional scheme since in the linear approach with the resting reference state SETTLS and traditional approach are equivalent).

3.1 The pressure instability

It is known that a correctly formulated SI scheme in σ coordinate shall have zero nonlinear residual for any choice of ${\pi_s}^*$ and therefore to be unconditionally stable. However, it was found that if true pressure based prognostic variable is rescaled by SI background pressure ($\hat{P} = \frac{p-\pi}{\pi^*}$) in the model formulation, then all terms, where this variable appears, create nonlinear residuals multiplied by a factor $\frac{{\pi_s}^*}{\overline{\pi_s}} - 1$ and the scheme is very unstable for any $\overline{\pi_s} \neq {\pi_s}^*$ (left plot on Figure 1).

We proposed a new true pressure based prognostic variable independent of the SI pressure ($\hat{q} = ln\frac{p}{\pi}$). We obtained an unconditionally stable SI scheme (right plot on Figure 1). Predictor-corrector scheme is then also unconditionally stable.

The PC scheme is stable for both variables as can be seen on Figure 1. But the convergence shown on Figure 2 is faster when the new prognostic variable $\hat{q}$ is used. The ICI scheme is convergent for any reasonable choice of ${\pi_s}^*$ and the PC scheme is sufficient to pacify the pressure related instabilities in a model formulated with η coordinate.

3.2 Temperature instability

The temperature instability was studied in η coordinate.

A similar behavior was found for the vertical velocity based prognostic variable rescaled by SI background values ($\hat{d} = -\frac{\pi^*}{RT^*}\frac{\partial w}{\partial ln\sigma}$). The artificial factor $\frac{T^*}{\overline{T}} - 1$ appeared in the non-linear residual,

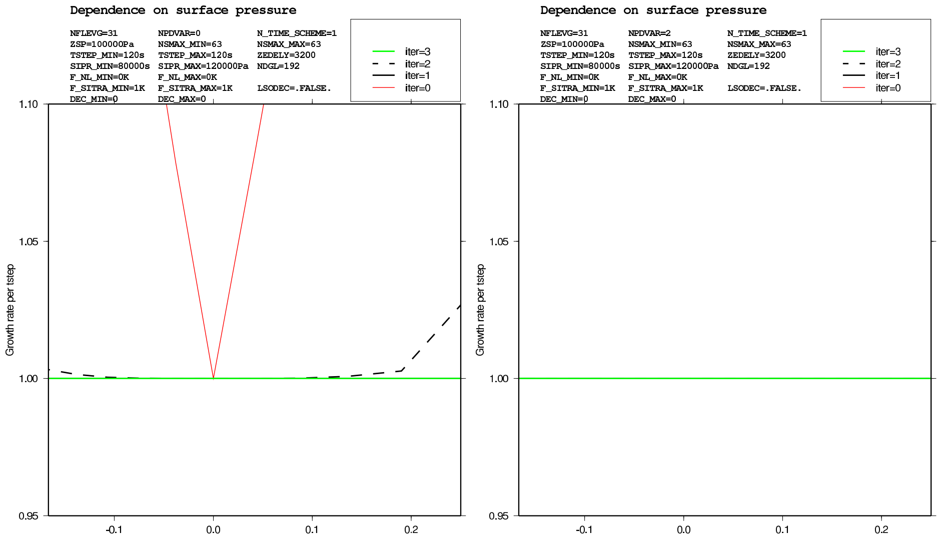

Figure 1: Dependency of the amplitude growth rate per time step upon the factor $\frac{\overline{\pi_s}-{\pi_s}^*}{{\pi_s}^*}$ (SI scheme - solid red line, PC scheme - solid black line, ICI scheme with 2 iterations - black dashed line and ICI scheme with 3 iterations - solid green line). New background state surface pressure is $\overline{\pi_s} = 1000hPa$. Calculated for horizontal wave number $k = 0.000625m^{-1}$, perfect temperature 239.5K, time step 120s and 31 σ levels. The formulation with $\hat{\mathcal{P}}$ is on the left and with $\hat{q}$ on the right.

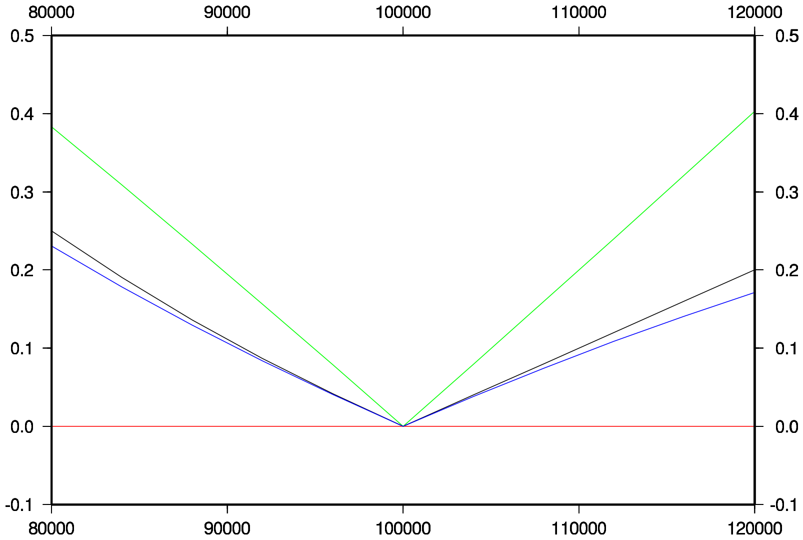

Figure 2: Dependency of $\rho(A)$ on ${\pi_s}^*$ ($\hat{\mathcal{P}}$+η - green line, $\hat{\mathcal{P}}$+σ - black line, $\hat{q}$+η - blue line, $\hat{q}$+σ - red line,) . Calculated for $\overline{\pi_s} = 1000hPa$, horizontal wave number $k = 0.000625m^{-1}$, perfect temperature 239.5K, time step 120s and 31 σ or 31 η levels

just due to scaling. A new prognostic variable was proposed, independent of SI background values ($d_3 = -\frac{p}{RT}\frac{\partial w}{\partial ln\sigma}$) (Bénard (2003)).

The 2TL SI NESC scheme is stable only in the case when $\overline{T} = T^*$ as shown on Figure 3. The 2TL PC NESC scheme is stable for the wider range of T^*. The model formulated with the d_3 variable converges faster for a wider range of T^* (Figure 4). As can be seen on Figure 4, the temperature instability is independent on the choice of the vertical coordinate. When $\Delta t \to \infty$ then the model formulated with the $\hat{d}$ variable converges only if $\overline{T} = T^*$ while the model formulated with d_3 converges for the interval $\frac{T^*}{2} < \overline{T} < 2T^*$.

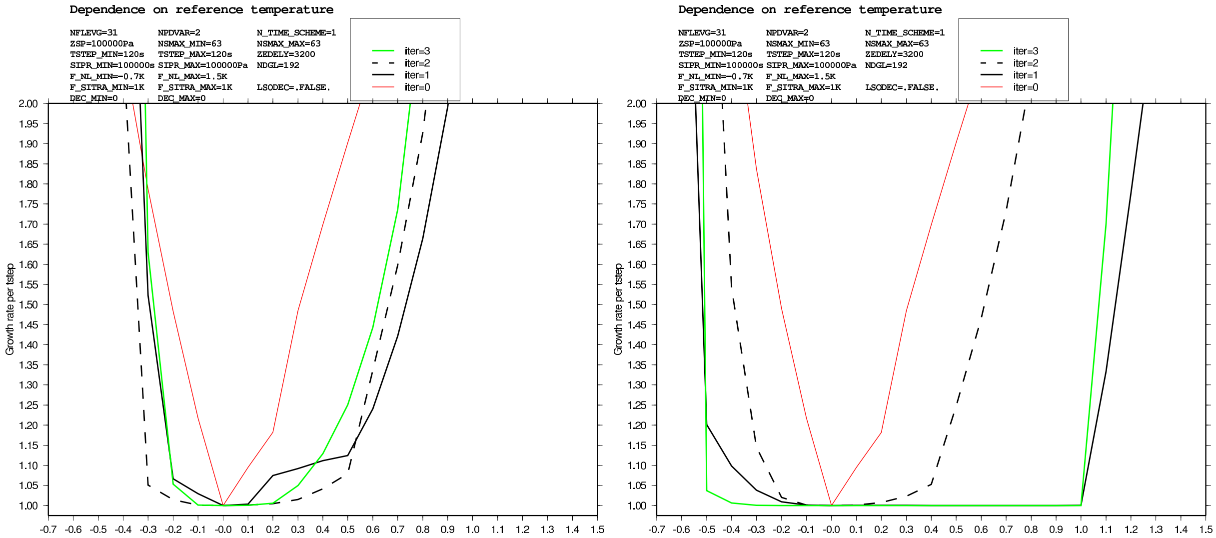

Figure 3: Dependency of amplitude growth rate per time step upon the factor $\frac{\overline{T}-T^*}{T^*}$ (SI scheme - solid red line, PC scheme - solid black line, ICI scheme with 2 iterations - black dashed line and ICI scheme with 3 iterations - solid green line). Calculated for $\overline{T} = 239.5K$, horizontal wave number $k = 0.000625m^{-1}$, perfect pressure 1000hPa, time step 120s and 31 η levels. The formulation with $\hat{d}$ on the left and with d_3 on the right.

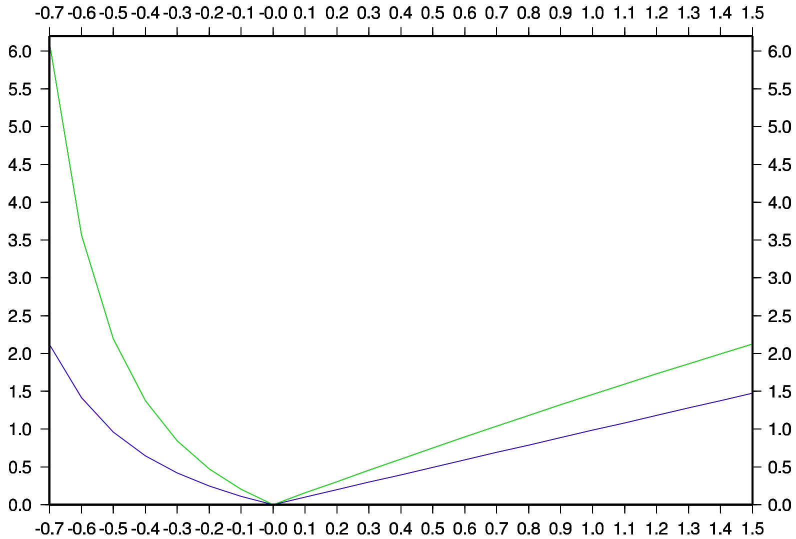

Figure 4: Dependency of $\rho(A)$ upon the factor $\frac{\overline{T}-T^*}{T^*}$ ($\hat{d}$+η - green line, $\hat{d}$+σ - black line, d_3+η - blue line, d_3+σ - red line,) . Calculated for $\overline{T} = 239.5K$, horizontal wave number $k = 0.000625m^{-1}$, perfect pressure 1000hPa, time step 120s and 31 σ or 31 η levels

3.3 Orography related instability

The instability related to orography has been studied experimentally. The 2d idealized flow over an Agnesi shaped mountain has been run for various values of the linearity parameter $C_l = \frac{Nh}{V}$. When $C_l << 1$ the flow is linear and for $C_l > 1$ the flow is highly non-linear. Here N is the constant

Brunt-Vaisala frequency of the atmosphere (set to $N = 0.1s^{-1}$) and the constant wind speed of the atmosphere $V = 10ms^{-1}$. Changing the height of the obstacle h, we can control the linearity of the flow regime. The obstacle half width was $L = 1000m$ and the flow regime was NH, because the non-dimensional quantity $C_h = \frac{NL}{V} = 1$.

The experiments were run in a domain with 128 points and quadratic truncation with horizontal resolution $dx = 200m$. The 100 vertical levels with approximate distance 300m were used. At the lateral boundaries Davies relaxation was implemented towards the initial state. At the top of the integration domain a sponge layer was implemented with the bottom at 12000m and the top at 29500m. The characteristic time of absorption was set experimentally to 200s. The top 14 levels were pure pressure levels and in the rest of the domain η levels were used. The SI reference temperature was set to 220K and the pressure to 1000hPa.

The mountain was inserted abruptly into the initial horizontal flow. The length of each test is characterized by non-dimensional number $t^* = \frac{tV}{L}$. The test was considered stable if it reached $t^* = 50$. If not then the scheme was considered to be unstable.

We tested the stability of the ICI scheme for various flow regimes ranging from the linear to the highly non-linear regime. We ran the tests for the values of $CFL = k_{max} V \Delta t$ from 0.1 up to 3. Our aim was to find the formulation of the PC scheme for which the non-linear flow regimes would be stable for higher values of CFL. Such situations are very often appearing in realistic simulations and the scheme that can be potentially exploited operationally should satisfy this kind of test.

We found that the 2TL SI and PC scheme with the prognostic variable d_3 and isothermal solver are unstable for the non-linear regimes and higher values of CFL (tables A and B). The non-linear regimes could be integrated only with the ICI scheme with 3 iterations.

The solution was proposed by Bénard. He proposed to use the prognostic variable

$$d_4 = d_3 + \frac{gp}{mRT} \vec{\nabla} \phi \frac{\partial \vec{v}}{\partial \eta}.$$

With this new prognostic variable the three-dimensional divergence yields $D_3 = D + d_4$ in the non-linear model and in the SI linear model as well. There remains no non-linear residual related to this elastic term. The results obtained with the SI NESC and PC NESC scheme run with isothermal SI scheme and the prognostic variable d_4 are in tables C and D. The SI NESC scheme remained unstable, but the PC NESC scheme was stable for the highly non-linear flow regimes for $CFL < 1.6$.

The results in tables A-D were computed with isothermal SI linear model. The results obtained with the SI NESC and PC NESC schemes with bi-isothermal model with $T^* = 300K$ and $T^*_a = 100K$ are in tables E and F. We see that even the 2TL SI scheme is stable for the all flow regimes. The PC scheme further improves the stability of the non-linear regimes for high values of CFL. The PC scheme is apparently more robust and it will be neccessity to use it when the small scale forcing from high resolution physics will become dominant and CFL will reach locally high values.

A

SI NESC scheme ($T^* = cst, d_3$)

CFL	1	0.8	0.6	0.4	0.1
2.1	2	2	2	2	2
1.6	2	2	2	2	2
1	2	2	2	2	2
0.3	1	1	1	1	1

B

PC NESC scheme ($T^* = cst, d_3$)

CFL	1	0.8	0.6	0.4	0.1
2.1	5	6	8	28	35
1.6	5	6	8	50	50
1	5	6	8	50	50
0.3	50	50	50	50	50

C

SI NESC scheme ($T^* = cst., d_4$)

CFL	1	0.8	0.6	0.4	0.1
2.1	2	2	2	3	3
1.6	2	2	2	2	2
1.0	1	1	1	2	2
0.3	1	1	1	1	1

D

PC NESC scheme ($T^* = cst., d_4$)

CFL	1	0.8	0.6	0.4	0.1
2.1	6	7	8	8	10
1.6	9	50	50	50	50
1.0	50	50	50	50	50
0.3	50	50	50	50	50

E

SI NESC scheme ($T^* \neq T_a^*, d_4$)

CFL	1	0.8	0.6	0.4	0.1
3.1	2	4	6	50	50
2.1	6	50	50	50	50
1.6	50	50	50	50	50
1.0	50	50	50	50	50
0.3	50	50	50	50	50

F

PC NESC scheme ($T^* \neq T_a^*, d_4$)

CFL	1	0.8	0.6	0.4	0.1
3.1	39	50	50	50	50
2.1	50	50	50	50	50
1.6	50	50	50	50	50
1.0	50	50	50	50	50
0.3	50	50	50	50	50

4 Accuracy aspects

4.1 Comparison to the analytical solution

To assess the accuracy of the scheme we ran the 3d idealized test over the Agnesi shaped circular mountain. It is the 3D generalization of the 2D test used in the previous section.

We computed the analytical solution using the theory of Smith (1980) assuming compressible and non-Bousinesque fluid. The analytical solution was obtained for the linear hydrostatic flow regime with $\overline{T} = 285K$, $V = 10ms^{-1}$, mountain height 50m, mountain half width 10km. The computation was carried out on the grid with the mesh isotropic size $dx = dy = 2km$ and the domain size 1024x1024 points with the quadratic truncation.

On Figure 5 the results obtained with the 2TL PC scheme with $\overline{T} = T^* = T_a^* = 285K$ is plotted. The model was integrated with a domain of 180x180 points, mesh size 2km and $\Delta t = 100s$. The Davies relaxation was used at the lateral boundaries and the sponge layer was implemented on the top of the model domain (with the bottom at 12570m and the top at 30000m). The relaxation time was 100s.

The results obtained with the 2TL PC scheme with $T^* = 300K$ and $T_a^* = 50K$ are shown on Figure 6.

The results are very close to the analytical values. The error maxima are less then 5%. The differences between the two experiments using different T_a^* and T^* values are negligible.

4.2 The accuracy of various formulations of the predictor

To assess the accuracy of the various formulations of the predictor we have run the warm and cold bubble test of Robert (1993). It is a non-stationary idealized test. We ran all the tests with the

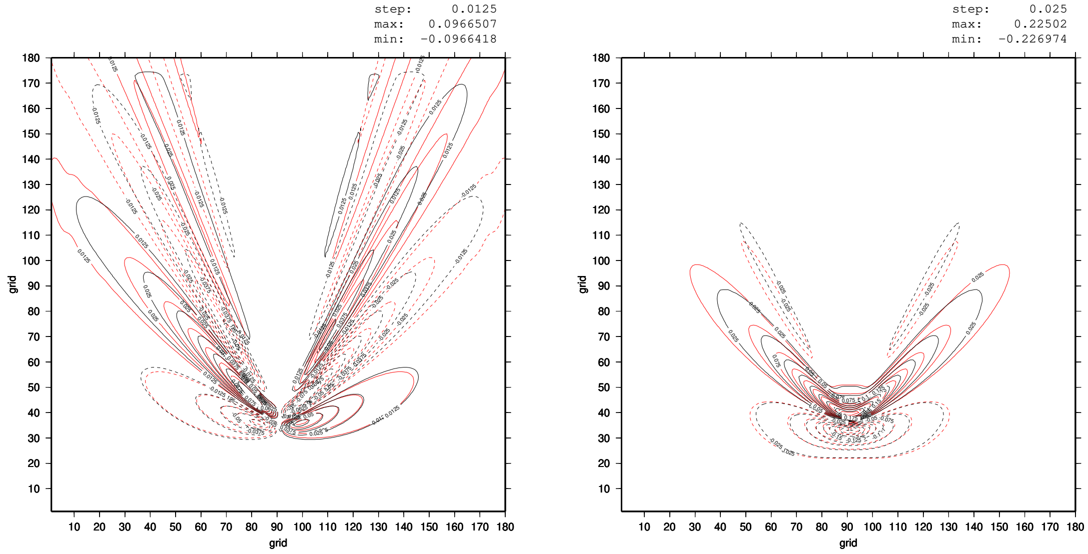

Figure 5: Linear hydrostatic flow over an Agnesi circular mountain. The analytical solution is plotted by red lines and the results obtained with 2TL PC scheme with $\overline{T} = T^* = T_a^* = 285K$ is plotted by the black line. The negative contours are dashed. The flow is from the bottom to the top. The u component of the wind is plotted on the left with contours $0.0125ms^{-1}$ and the perturbation of v from the background value $V = 10ms^{-1}$ is plotted on the right with contours $0.025ms^{-1}$

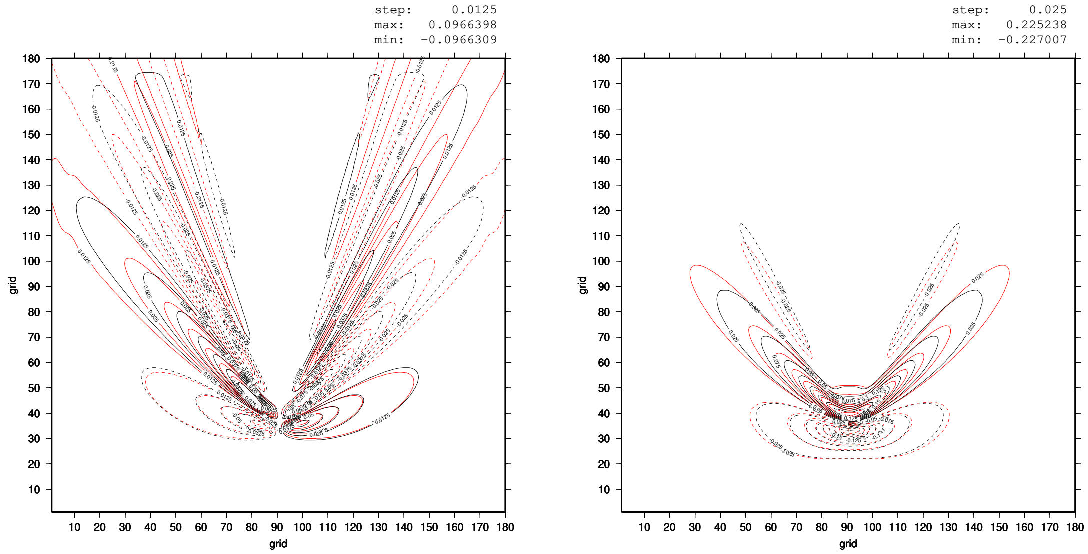

Figure 6: the same as on Figure 5 but for the 2TL ICI scheme with $T^* = 300K$ and $T_a^* = 50K$

prognostic variable d_3, because all the versions of predictor were not yet implemented in the model for d_4 and since the test is without orography the model is sufficiently stable with d_3 as well. The model

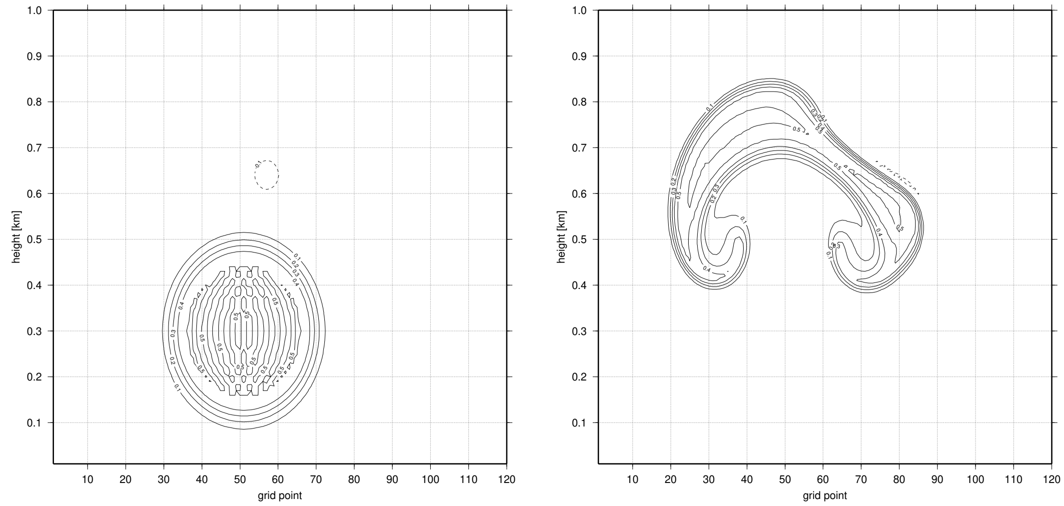

Figure 7: The perturbation of potential temperature of warm and cold bubble test obtained by reference run (ICI scheme with 3 iterations). The initial state is plotted on the left plot and the state after 420s is on the right plot.

description is provided in Robert (1993).

The reference experiment was run with the ICI NESC scheme with three iterations with a very short $\Delta t = 0.2s$ up to $t = 420s$. The initial state and the state at the end of the integration are plotted on Figure 7. The solution is almost identical to one published by Robert (1993). The reference experiment was run with $T^* = 350K$, $T_a^* = 50K$. The quadratic grid was used with 120 points with mesh size 10m and 120 vertical levels of approximative distance 10m.

The set of tests was then run with the 2TL SI, 2TL PC and 2TL ICI scheme with 7 iterations with various formulations of the predictor (NESC,SETTLS or traditional) with $\Delta t = 5s$. On Figure 8 is plotted the standard deviation of the perturbation of the potential temperature computed from the difference between the experiment and the reference run.

It is apparent that for this test the SI NESC scheme is very inaccurate. The traditional SI scheme is more accurate then the SI SETTLS scheme. The PC NESC is more accurate then any SI scheme. The PC SETTLS and PC traditional perform almost identically. We see from the results obtained with the ICI scheme with 7 iterations that the ICI scheme is convergent and that the solution is independent on the predictor formulation.

5 The Lothar storm case study - the properties of the Rossby-Haurwitz modes

To test the accuracy of the model for synoptic scales the Lothar storm case was chosen. It is the first of the two storms from December 1999 that passed over Europe during Christmas. The meso-cyclone formed over Atlantic Ocean and it moved rapidly towards Europe. During the 26th of December 1999 the storm hit France, Germany, Switzerland and Italy and caused severe damages. Operational forecast of the global model ARPEGE provided reasonable guidance for Lothar storm. When ALADIN

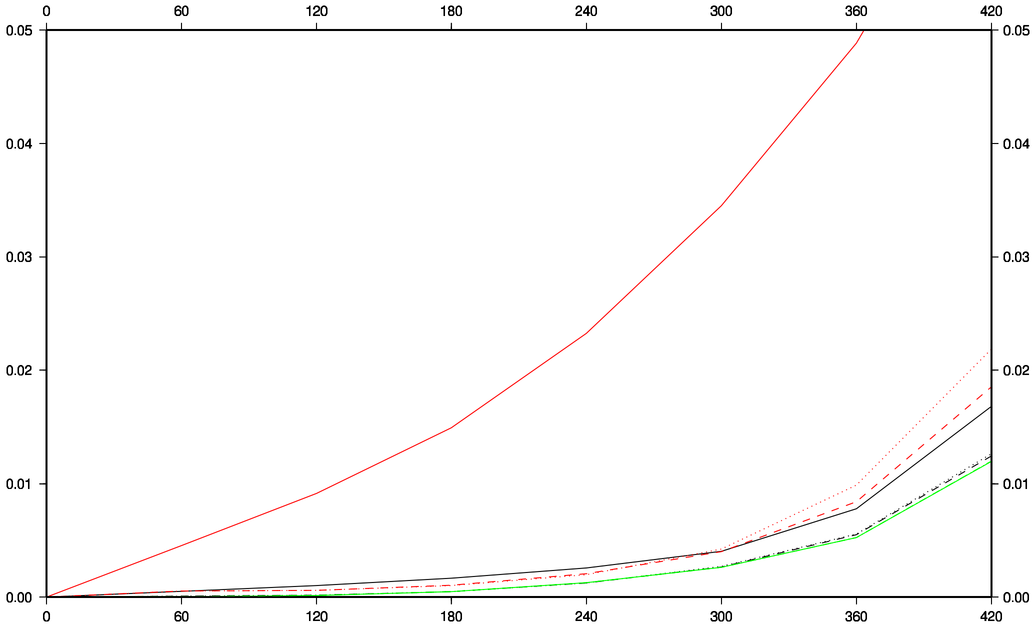

Figure 8: The evolution of standard deviation of the perturbation of potential temperature computed against the reference run. The results are obtained for 2TL SI scheme (red lines), 2TL PC scheme (black linear) and ICI scheme with 7 iteration (green lines). The schemes with NESC extrapolations are plotted by solid lines, with SETTLS extrapolation by dotted lines and with traditional extrapolation by dashed lines.

is coupled with ARPEGE prediction using quadratic coupling or 3 hour frequency coupling, the prediction of Lothar storm is sufficiently accurate to be considered successful in the view of current LAM performance. On Figure 9, we can see the 26th and 27th December 1999 analysis of model ARPEGE.

The Lothar storm is possible to predict using the dry adiabatic model version. However, such prediction is not possible to verify against the model analysis. Therefore we used the diabatic version of model ALADIN. We ran the prediction using initial conditions from 12 UTC on the 25th of December 1999. The reference run was obtained with the hydrostatic model version using the 2TL SI SL scheme with SETTLS extrapolation (Figure 10). The integration domain was the ALADIN/LACE domain, the horizontal mesh size is 12.2km and $\Delta t = 600s$. The position of the cyclone is shifted slightly to the east and is 1hPa shallower (972hPa in the center) then in the analysis (the left plot on Figure 9).

The physics in ICI scheme was called once per time step, during predictor. The physical tendencies were considered to be valid at departure point of SL trajectories at time instant t.

We have integrated the Lothar case using the NH version of model ALADIN. We used the prognostic variable d_4 and we set $T_a^* = 50K$ and $T^* = 350K$. We used the 2TL ICI NESC with SL advection. The results are showed on Figure 11. Comparing to the analyses, there is an underestimation of the minimum MSLP by 2 hPa. This difference is reduced to 1hPa after the first iteration of ICI scheme. The results obtained with the NH model version are almost identical to the reference hydrostatic model results. This proves that the tested scheme applied on ALADIN's NH dynamics efficiently stabilises all the possible sources of instabilities for the "hydrostatic" time step length (orographically induced waves, SHB temperature and pressure instabilities), while keeping the quality of the simulation of the large scales as in the hydrostatic model. We can deduce from Figure 11, that the PC scheme is fully sufficient to integrate the model for resolution around 10km, because there is no significant change in

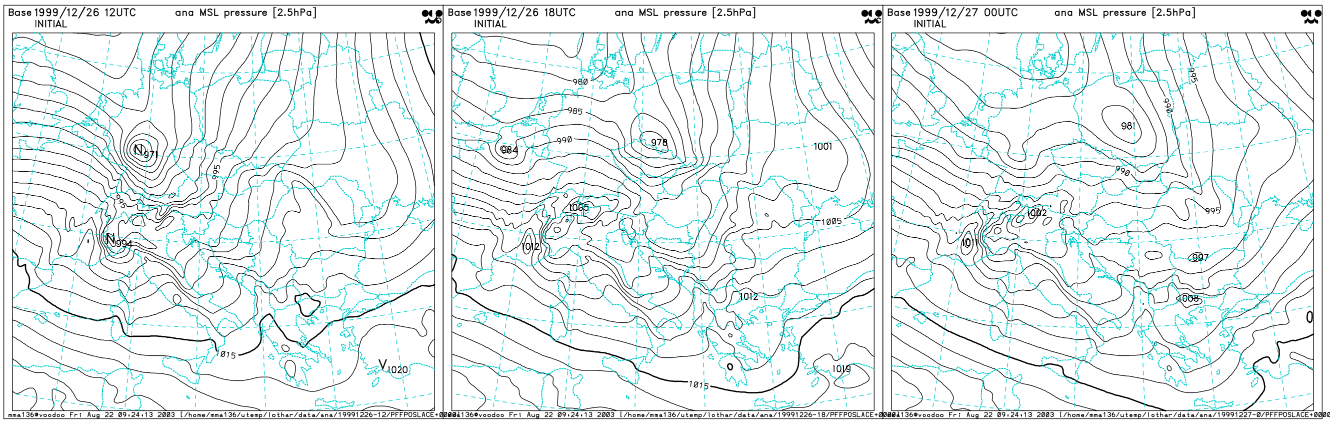

Figure 9: The 3DVAR analysis of model ARPEGE, for the Lothar storm case from the 26th of December 1999. The MSLP is plotted with contour interval 2.5hPa. The storm moved eastward over France, Germany (left and middle plot) and finally during the 27th of December 1999 it weakened over southwest Poland (right).

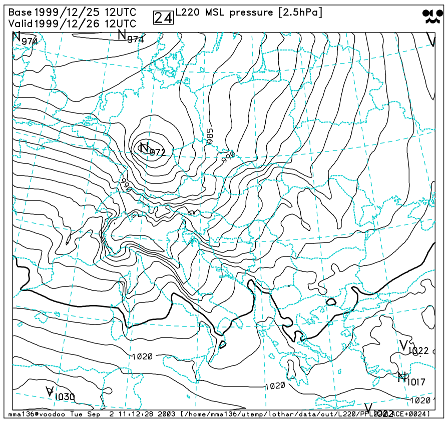

Figure 10: The 24h reference prediction of Lothar storm from 25th of December 1999 12UTC. The prediction was obtained with the hydrostatic model version with 2TL SI SL LSETTLS scheme.

the results when using two or more iterations of the SI solver.

Our aim was to show that the 2TL ICI scheme doesn't deteriorate results obtained with the standard SI scheme when applied to a synoptic scale case. The linear analysis indicated that the Rossby-Haurwitz (RH) modes are slightly sped up by the 2TL PC scheme. The frequencies of the RH modes are 0.1% greater than their analytical value. However, there are still nonlinear residuals not included in the analysis and a case study with the full nonlinear model has to be carried out to draw a final conclusion.

The results obtained with the 2TL ICI SL non-extrapolating scheme with NH version are almost equivalent to the reference results from the hydrostatic model integrated using the 2TL SI SL LSETTLS scheme at the 10km scale. This confirmed that the partially implicit treatment of RH modes in ICI scheme doesn't deteriorate them.

The simulations using the NH model version further proved that the methods used to stabilise acoustic modes and the orographically induced instabilities are neutral to RH modes. The Lothar case study proved that for resolutions around 10km the 2TL SL PC non-extrapolating scheme without additional filtering is sufficient to integrate the NH model ALADIN formulated with the prognostic variables d_4 and $\hat{q}$. No significant improvement can be gained by additional iterations of the SI solver.

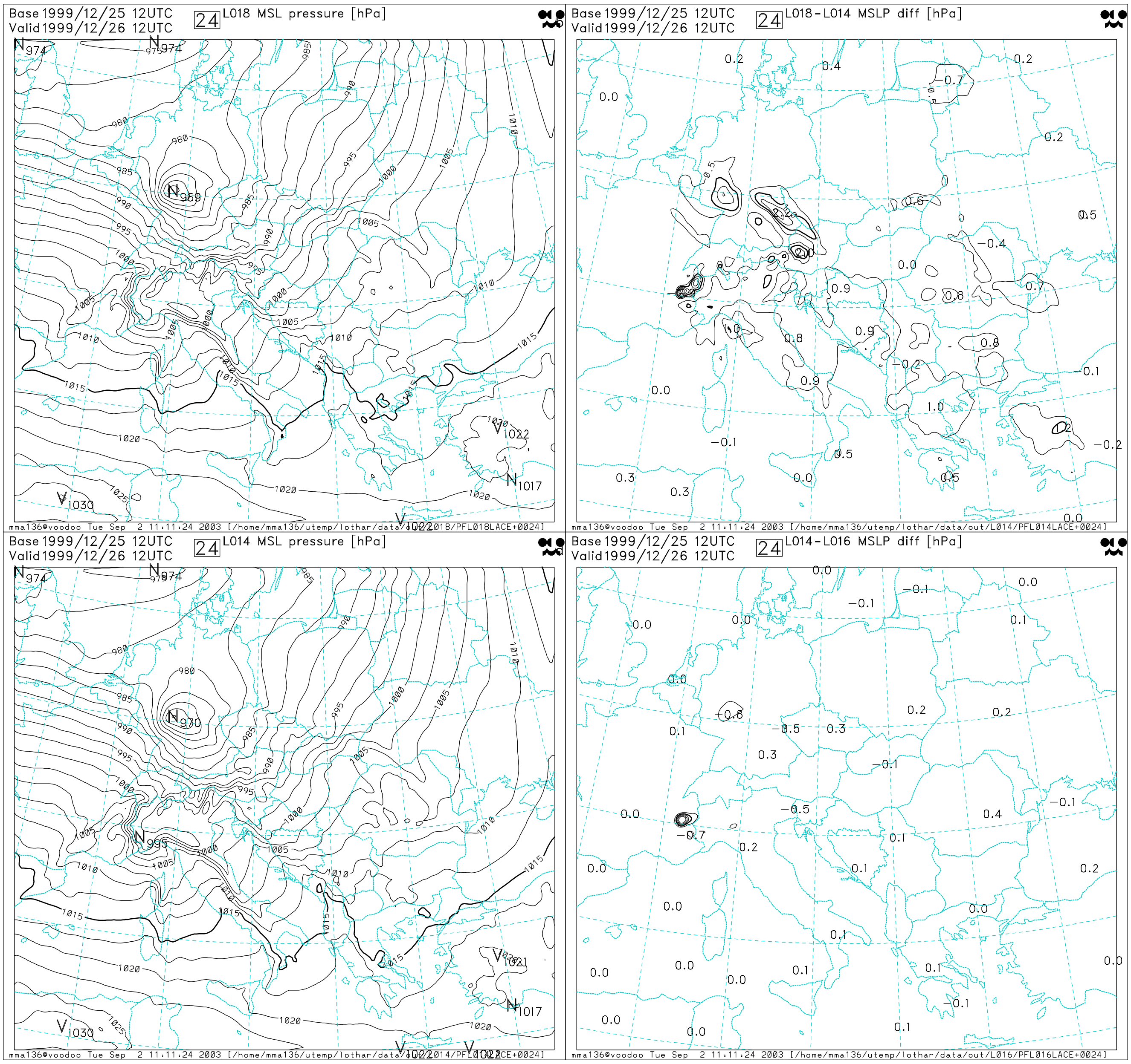

Figure 11: The 24h prediction from 25th of December 1999 12UTC obtained with the 2TL ICI SL non-extrapolating scheme with n=0 (top left plot) and n=1 (bottom left plot). The differences between the runs with different number of iterations of ICI scheme are plotted in the right column. The differences between the SI scheme and the PC scheme runs are on top right plot, and the differences between the PC scheme and ICI scheme with n=2 are on the bottom right plot

References

[1] Bénard, P., 2003: Stability of semi-implicit and iterative centred-implicit time discretization for various equations systems used in NWP, to be published in MWR

[2] Bénard, P., 2003: On the use of a wider class of linear systems for the design of semi-implicit time-schemes in NWP, to be published in MWR

[3] Bénard, P., R. Laprise, J. Vivoda and P. Smolíková, 2003: Stability of leap-fog constant-coefficient semi-implicit schemes for the fully elastic system of Euler equations. Flat-terrain case. Accepted in MWR

[4] Bubnová, R., G. Hello, P. Bènard and J.-F. Geleyn, 1995: Integration of the fully elastic equations cast in the hydrostatic pressure terrain-following coordinate in the framework of the ARPEGE/ALADIN NWP system. Mon. Wea. Rew., 123, 515-535

[5] Cullen, M.J.P., 2001: Alternative implementations of the semi-Lagrangian semi-implicit schemes in the ECMWF model. Q.J.R. Meteorol. Soc., 127, 2787-2802

[6] Golding, B.W., 1992: An efficient non-hydrostatic model. Meteor. Atmos. Phys., 50, 89-103

[7] Laprise, R., 1992: The Euler equations of motions with hydrostatic pressure as an independent variable. Mon. Wea. Rew., 99, 32-36

[8] Robert, A., J. Henderson and C. Turnbull, 1972: An implicit time integration scheme for baroclinic models of the atmosphere. Mon. Wea. Rev., 100, 329-335

[9] Robert, A., 1993: Bubble convection experiments with a semi-implicit formulation of the Euler equations. J. Atmos. Sci., 50, 1865-1873

[10] Simmons, A.J., B.J.Hoskins and D.M.Burridge, 1978: Stability of the semi-implicit method of time integration. Mon. Wea. Rew., 106, 405-412

[11] Temperton, C. and A. Staniforth, 1987: An efficient two-time level semi-Lagrangian semi-implicit integration scheme. Q.J.R. Meteorol. Soc., 113, 1025-1039

[12] Qian, J.-H., F.H.M. Semazzi and J.S.Scroggs, 1998: A global non-hydrostatic semi-Lagrangian atmospheric model with orography. Mon. Wea. Rew., 126, 747-771

[13] Smith, R.B., 1980: Linear theory of stratified hydrostatic flow past an isolated mountain. Tellus, 32, 348-364